

Supersoft X-ray Sources. Basic Parameters.

V.F.Suleimanov¹, A. A. Ibragimov¹,

1 - Kazan State University, Kazan, Tatarstan, Russia

Received March 5, 2002; in final form, October 10, 2002

Abstract

The parameters of ten supersoft X-ray sources (RX J0439.8-6809, RX J0513.9-6951, RX J0527.8-6954, CAL 87, CAL 83, 1E 0035.4-7230, RX J0048.4-7332, 1E 0056.8-7154, RX J0019.8+2156, RX J0925.7-4758) observed by ROSAT obtained using blanketing approximations and LTE model atmospheres are analyzed. The consistency of the resulting parameters with a model with stable/recurrent burning on the surface of the white dwarf is studied. The luminosity and sizes of seven of the sources are in good agreement with this model. The masses of the white dwarfs in these sources are estimated. A formula that can be used to estimate the masses of white dwarfs in classical supersoft sources based on their effective temperatures is presented.

1. Introduction

Supersoft X-ray sources are a class of X-ray object with very soft spectra (effective temperatures of the order of 10 - 80 eV) (Kahabka & van den Heuvel 1997). It is known that supersoft sources do not form a uniform class. Some are close binary systems with periods from tenths of days ($0^d.17$ for 1E0035 - typical of the periods of cataclysmic variables) to several days ($1^d.04$ for CAL83).

The widely adopted classical model for these sources put forth by van den Heuvel et al. (1992, vdH92) proposed that they are close binary systems with a white dwarf and subgiant, in which material from the donor is accreting onto the white dwarf on the thermal time scale at a rate on the order of 10^{-7} M/yr. At such accretion rates onto the white-dwarf surface, a regime of stable thermonuclear hydrogen burning is realized, without the substantial increase in the radius of the white dwarf predicted theoretically by Paczynski & Zytlow (1978), Iben (1982), Nomoto (1982), Fujimoto (1982), Iben & Tutukov (1996). However, this model also encounters certain difficulties. In particular, the radial velocities of the source CAL87 imply a mass for the secondary that is half that of the white dwarf, in contradiction with the expectations of the model (Cowley et al. 1998).

Symbiotic stars with periods of hundreds of days (~ 550 d for AG Dra) are also found among supersoft sources. It is thought that, in these systems, there is accretion from the wind of a giant donor, with subsequent burning on the white-dwarf surface. It is likely that recurrent novae (such as U Sco (Kahabka et al. 1999a)) also undergo a supersoft stage. The source RX J0439 in the Large Magellanic Cloud has not yet been demonstrated to be a binary. There are no signs of an accretion disk in its spectrum, so that it has been classified either as a single star at a very late stage of evolution or as a system of two degenerate dwarfs (Gansicke et al. 2000).

In all cases, the presence of soft X-ray emission is associated with thermonuclear burning on the surface of a white dwarf or a naked hydrogen or helium core of a star in a late stage of evolution.

In the first part of our current study (Ibragimov et al. 2003), we approximated ROSAT spectra using blanketed LTE model atmospheres. Here, we analyze the consistency of those

results with the theory of stable/recurrent burning on the surface of a white dwarf, estimate a number of physical parameters of the sources, and analyze their mass–effective temperature relation. The full designations of the sources are presented in Table 1. We will use shortened designations consisting only of the first several symbols.

2. Position of sources in the Hertzsprung - Russel diagram

In previous paper (Ibragimov et al. 2003), we approximated archival ROSAT observations using blanketed LTE model atmospheres. For most sources, we obtained four different approximations: for the smallest and largest possible values of $\log g$ and with the column density of interstellar hydrogen either treated as a free parameter or fixed at the Galactic value (i.e., the value for the given direction in the Galaxy). The resulting source parameters are presented in Tables 3 - 6 of Ibragimov et al. (2003): the column density of interstellar hydrogen N_H , effective temperature T_{eff} , logarithm of the gravitational acceleration $\log g$, and normalization factor R^2/d^2 . Knowing the source parameters and distances d , we can find their luminosities and sizes:

$$L = 4\pi\sigma T_{\text{eff}}^4 \frac{R^2}{d^2} d^2, \quad R = \sqrt{\frac{R^2}{d^2}} d. \quad (1)$$

We took the distances to the Large and Small Magellanic Clouds to be 50 and 60 kpc, respectively. We calculated the luminosities and sizes of sources in the Galaxy assuming $d = 2$ kpc.

The positions of sources in the Hertzsprung - Russell (HR) diagram are shown in Fig. 1, which also depicts theoretical curves for white dwarfs of various masses with hydrogen burning on their surfaces. It is known (Iben & Tutukov 1996) that the maximum luminosity of such a white dwarf depends substantially on its internal temperature, especially in the case of low-mass white dwarfs. The luminosity of a hot white dwarf whose temperature is comparable to the temperature in a shell with thermonuclear burning,

$$\frac{L}{L_{\odot}} = 60000 \left(\frac{M}{M_{\odot}} - 0.52 \right), \quad (2)$$

is substantially lower than the luminosity reached in the case of thermonuclear burning on the surface of a cooled white dwarf,

$$\frac{L}{L_{\odot}} = 46000 \left(\frac{M}{M_{\odot}} - 0.26 \right). \quad (3)$$

Since we do not know the temperatures of the white dwarfs in the studied sources a priori, we compared their positions in the HR diagram with evolutionary tracks for novae in the declining brightness phase, which corresponds to burning on the surfaces of cool white dwarfs (Kato & Hachisu 1994) (Fig. 1a), and with tracks for burning on the surfaces of hot white dwarfs, above the edge of the stable-burning strip (Iben & Tutukov 1996) (SBS; the zone in which there can be continuous burning; Fig. 1b). The horizontal part of the tracks reflects variations in the photospheric radius and effective temperature of the white dwarf with the luminosity remaining nearly constant at its maximum value, while the sloped part of the tracks (Fig. 1a) reflects variations in the luminosity as the temperature of the white dwarfs decreases, with the radius remaining constant.

Four sources (RX J0925, CAL 87, RX J0513, and 1E 0056) are located near turning points of the evolutionary curves for both cool and hot white dwarfs. This means that they are located

in the SBS, and that their luminosities are close to the maximum values (without appreciable increases in the white-dwarf radii). Note that their positions correspond to curves for white dwarfs of various masses, depending on their internal temperatures (compare Figs. 1a and 1b). Three sources (CAL 83, RX J0527, and 1E 0035) are located on white-dwarf cooling curves below the SBS.

The positions of four sources (1E 0035, 1E 0056, CAL 83, and RX J0527) are shown for two values of $\log g$ (the lower left point corresponds to $\log g = 9.5$, and the upper right point to $\log g = 8.0$). Since the parameters obtained for RX J0048, RX J0439, and RX J0019 were either uncertain or do not agree with acceptable parameters for white dwarfs, these objects are shown only in Fig. 1a for the minimum value of $\log g$. The luminosity of RX J0019 is very uncertain, but this source may be a white dwarf located in the SBS. RX J0439 and RX J0048 have luminosities higher than the Eddington luminosities of white dwarfs (a lower limit for the latter source is indicated).

The parameters obtained in (Ibragimov et al 2003) show a large scatter due to uncertainty in the interstellar absorption (determined by N_H). However, independent estimates of N_H derived from ultraviolet observations are available for some of the sources, which testify that the values of N_H in the direction of the sources in the Magellanic Clouds differ little from the Galactic value. Therefore, we used the parameters for these sources obtained for the Galactic value of N_H (when this was possible). The values of the approximation parameters adopted to obtain the source characteristics are presented in Table 1. A basis for the choice of one or another approximation for each source is given below.

3. Estimates of the source masses and sizes

Figure 2 shows the positions of the sources in the $R - \log g$ plane. The bold line presents the theoretical dependence for cool white dwarfs, while the dashed line presents the same dependence for the case when the white-dwarf radius is twice the theoretical value for a cool white dwarf. The circles in Fig. 2a show the positions of six sources: three with fixed values of $\log g$ (CAL 87, RX J0925, and RX J0513) and three whose sizes are very uncertain (RX J0019) or are not consistent with the sizes expected for white dwarfs (RX J0439 and RX J0048); only lower limits to the sizes of these last sources are indicated. The circles in Fig. 2b show the positions of the remaining four sources for the extreme values of $\log g$.

Let us analyze the positions of the sources in the HR diagram (Fig. 1) and in the $R - \log g$ plane (Fig. 2) taking into account available observational information, with the aim of estimating the masses of the white dwarfs in these objects. The mass can be derived from the source size as follows. We first determine the regions of $\log g$ values in Fig. 2 corresponding to the sizes of the sources, to the theoretical sizes of cool white dwarfs (solid line), and to sizes exceeding these theoretical sizes by a factor of two (dashed line; we will call this the "2R case"). In this way, we find the $\log g$ values for which the theoretical curves correspond to the source sizes derived from observations. We can then find the mass of an object from the two $M - \log g$ relations, calculated from the $M - R$ law for cool white dwarfs (Popham & Narayan 1995) and for objects with the same masses but doubled radii (Fig. 3).

RX J0439.8-6809. The size and luminosity of this source testify that it is not a classical supersoft source. In our analysis, we used the parameters derived for $\log g = 7.5$ and the Galactic N_H value, since N_H values derived independently using Hubble Space Telescope (HST) data (Gänsicke et al. 2000) demonstrate the soundness of this approach. Two models are currently being considered for this source in the literature. It may be a system of two degenerate dwarfs, one of which overfills its Roche lobe, while thermonuclear burning occurs on the surface of the

other (Iben & Tutukov 1993), or it may be a star such as PG 1159, which is the virtually naked core of a star in a late stage of its evolution (Gänsicke et al. 2000). In either case, the spectrum of this source cannot be modeled using hydrostatic model atmospheres with solar chemical composition, and the parameter values we have obtained should be treated as very approximate. It is not possible to derive its mass from our data.

RX J0513.9 - 6951. This is a recurrent binary whose parameters are in agreement with the vdH92 model. The value of N_H has been derived using HST data (Gänsicke et al. 1998), making it possible to determine its physical parameters. We used the parameters derived for the Galactic N_H value as upper limits for the luminosity and radius and a lower limit for T_{eff} , and used the parameters derived allowing N_H to be free for the opposite limits. The location of the source in the HR diagram is near the turning points of evolutionary tracks with masses of 1.1 - 1.2 M_\odot for hot and 0.8 - 0.9 M_\odot for cool white dwarfs. Its size corresponds to the theoretical radius of white dwarfs with masses of 0.6 - 0.7 M_\odot , or 1 - 1.3 M_\odot for the 2R case. The source size exceeds the size of a cool white dwarf, and its mass lies in the range 0.8 - 1.2 M_\odot .

RXJ0527.8-6954. The X-ray flux from this object continually decreased in the 1990s, but the source was not detected by the Einstein satellite 20 years ago, although it was in its field of view (Greiner et al. 1991, 1996). It thus appears that the source is recurrent and was in a declining brightness phase during the ROSAT observations. We used the parameters obtained for the Galactic N_H , since the approximation data obtained when N_H was allowed to float are very uncertain. The source occupies the position of cooling curves for white dwarfs with masses of 1.2 - 1.4 M_\odot in the HR diagram. Its position in the $\log g - R$ plane is in better agreement with the relation for a cool white dwarf with $\log g = 9.5$, which yields a mass based on its size of 1.3 - 1.4 M_\odot . Thus, the $\log g$ of the source is fairly high (about 9.5) and its mass is in the range 1.2 - 1.4 M_\odot .

CAL 87. This object is an eclipsing binary system that has been studied by various authors and observed by various satellites (Hartmann & Heise 1997, Parmar et al. 1997, Asai et al. 1998). The N_H value is appreciably higher than the Galactic value, presumably due to the fact that the orbital plane is strongly inclined to the line of sight, and the X-ray source is partially eclipsed by material above the plane of the disk. Its parameters are well defined, since it has a hard spectrum. The position of the object in the HR diagram suggests that the N_H value in the direction of the source may be overestimated, so that its luminosity and size are likewise overestimated. We therefore considered only the lower limits of these quantities. The source is located in the HR diagram in the SBS near white dwarfs with masses of 1.1 - 1.3 M_\odot . Its size is in agreement with theoretical radii of white dwarfs with masses lower than 1.05 M_\odot (1.3 M_\odot for the 2R case). Consequently, the size of the source exceeds those of cool white dwarfs, and its mass is in the range 1.1 - 1.3 M_\odot .

CAL 83. This is a classical double supersoft source. We used the parameters obtained for the Galactic N_H value, since the absorption for this object derived from HST observations is close to this value (Gänsicke et al. 1998). The source is located in the HR diagram below the SBS on the cooling curves for white dwarfs with masses of 0.8 - 1.1 M_\odot (for $\log g = 8.0 - 9.5$). Its position in the $\log g - R$ plane is in agreement with the size of a cool white dwarf with a low $\log g$ (about 8.0). The mass derived from the size corresponds to 0.6 - 0.8 M_\odot (1.2 - 1.3 M_\odot for the 2R case). Thus, our estimates suggest the mass is close to 0.8 M_\odot .

1E 0035.4 - 7230. This is a cataclysmic variable that probably has a complex history (Kahabka & Ergma 1997). We derived parameters for two separate observations, which are in good agreement with each other. We used the parameters obtained when approximating the April 28, 1992 observations using the Galactic N_H value. The source is located in the HR

diagram below the SBS on cooling curves for white dwarfs with masses 0.8 -1.0 M_{\odot} . Its size is in agreement with that for a cool white dwarf with a mass of about 0.75 M_{\odot} (1.25 M_{\odot} in the 2R case). Consequently, the size and position of the source in the HR diagram indicate the low value $\log = 8.0$ and a mass of 0.7 - 0.8 M_{\odot} .

RX J0048.4-7332. This is a symbiotic novae that has been in a flaring stage since 1981 (Morgan 1992). Our hydrostatic models yield high luminosities and sizes that are not consistent with the vdH92 model. However, models with winds ($\dot{M} \sim 10^{-5} - 10^{-6} M_{\odot}/\text{yr}$) yield reasonable estimates of the source's luminosity (Jordan, et al, 1996). The parameters we have determined should be treated as estimates. We are not able to determine the source's mass.

1E 0056.8-7154. This is the nucleus of the planetary nebula N67. We obtained parameters for two observations that were not in good agreement, although the confidence contours for the two observations are consistent with each other; i.e., there is a high probability that the parameters obtained from the second observation are also possible for the first observation. In our analysis, we used the parameters derived for the October 7, 1993 observation leaving N_H free to vary with $\log g = 8.0$. The object is located in the SBS for white dwarfs with masses of 0.9 - 1.1 M_{\odot} (hot white dwarfs) and 0.5 - 0.8 M_{\odot} (cool white dwarfs).

Its size exceeds the sizes of cool white dwarfs and is consistent with the 2R case if the mass is lower than 1.0 M_{\odot} . It is probable that the white dwarf is hot, has recently formed (the planetary nebula), and has a mass of 0.9 - 1.1 M_{\odot} .

RX J0019.8+2156 or QR And. This is a Galactic supersoft source. We used the parameters obtained leaving the N_H value free with $\log g = 7.5$, since the parameters derived for the Galactic N_H value yield a very low luminosity ($\sim 2 \cdot 10^{34} \text{erg}/\text{sd}(\text{kpc})^2$) and size ($4 \cdot 10^7 \text{cm} \text{d}(\text{kpc})$) for the source. The results are very uncertain, but in good consistency with the vdH92 model. We are not able to estimate the source mass using the available data.

RX J0925.8-6809. This is also a Galactic supersoft source located behind a molecular cloud in Vela, so that it is strongly reddened ($E(B - V) = 2.1$) (Motch et al. 1994). We adopted a distance of 2 kpc, since this yields good agreement with the vdH92 model. In this case, the source is located above the SBS, and its mass is 1.2 - 1.4 M_{\odot} . Its size is also consistent with this mass estimate (larger than 0.95 M_{\odot} for a cool white dwarf and larger than 1.25 M_{\odot} for the 2R case). The size of the white dwarf is larger than expected for a cool white dwarf.

Thus, we have estimated the white-dwarf masses and the most probable values of the remaining physical parameters for seven supersoft sources (Table 2). Of these, four sources (CAL 87, RX J0925, 1E0056, and RX J0513) were in the SBS at the epoch of observation, with their sizes exceeding those of cool white dwarfs. The remaining three sources (CAL 83, RX J0527, and 1E0035) were below the SBS on white-dwarf cooling curves, with their sizes consistent with those of cool white dwarfs.

We conclude that the physical characteristics of classical supersoft sources are consistent with the model of stable or recurrent thermonuclear burning on the surface of a white dwarf and that these sources occupy positions in the HR diagram either near the turning points of evolutionary tracks for this model or lower, on white-dwarf cooling curves.

4. Mass — temperature relation

Let us investigate the relation between the effective temperature of the supersoft sources and the corresponding white-dwarf masses. It is known (Iben & Tutukov 1996) that the luminosity of a white dwarf with thermonuclear burning on its surface is located on the horizontal section, or plateau, of the theoretical curves in the HR diagram associated with their mass (formulas (2) and (3)). Using a linear approximation for the mass — radius dependence for white dwarfs

and relation (3) between the luminosities and masses of white dwarfs, Iben and Tutukov (Iben & Tutukov 1996) derived the dependence of the maximum possible effective temperature T_{eff} on the white-dwarf mass:

$$T_{\text{eff}} = 3.6 \cdot 10^5 K \frac{(M/M_{\odot} - 0.26)^{1/4}}{(1 - 0.59M/M_{\odot})^{1/2}}, \quad (4)$$

shown in Fig. 4 by the dotted curve. This formula was derived assuming that the maximum temperature is reached when the luminosity is half the luminosity on the plateau (3), and the photospheric radius is double the radius of the white dwarf.

This same figure presents the positions of the four sources located in the SBS and two theoretical dependences. The upper curve is constructed from the positions of the maximum-temperature points for the evolutionary tracks of novae in the declining brightness phase (Kato & Hachisu 1994), and the lower curve from the positions of these points for hot white dwarfs with a shell burning source (Iben & Tutukov 1996). It is clear that the formula proposed in (Iben & Tutukov 1996) does not provide a good description of the relation between the mass and maximum temperature of the supersoft sources, although its underlying principle remains correct. We attempted to improve this formula by allowing for the fact that the mass — radius relation for white dwarfs is not linear, and the ratio of the size of the photosphere of a supersoft source to the radius of the corresponding cool white dwarf could depend on its mass. We accordingly approximated the mass — radius relation using a third-order polynomial:

$$\frac{R}{R_{\odot}} = 0.0273 - 0.0417 \frac{M}{M_{\odot}} + 0.0364 \left(\frac{M}{M_{\odot}} \right)^2 - 0.0138 \left(\frac{M}{M_{\odot}} \right)^3, \quad (5)$$

and used this in place of the linear relation. However, Accordingly, we propose the following formula for this significantly influenced the results only for white the relation between the mass of a white dwarf and its dwarfs with masses higher than $1.2 M_{\odot}$. Analysis of the ratio of the photospheric radius to the white- dwarf radius indicated that, in order to construct the best approximation to the results of the computations of surface thermonuclear burning, this ratio should be inversely proportional to the square of the white dwarf mass.

Analysis of effective temperature in the region of the SBS:

$$T_{\text{eff}} = 3 \times 10^5 K \frac{M/M_{\odot}(M/M_{\odot} - 0.26)^{0.25}}{(1 - 1.53M/M_{\odot} + 1.33(M/M_{\odot})^2 - 0.51(M/M_{\odot})^3)^{0.5}}. \quad (6)$$

This relation is shown in Fig. 4a by the dashed curve. We can see that it provides a good approximation to the results of the numerical computations. It was obtained assuming that the luminosity of the white dwarf is half the luminosity on the plateau, and the photospheric radius is a factor of $2(M_{\odot}/M)^2$ larger than the white-dwarf radius. We note that this is only a suggestion for the required relation, and the actual relation at the boundary of the SBS could be more complex.

Figure 4b shows the positions of the remaining three sources (CAL 83, 1E 0035, and RX J0527) in the $M - T_{\text{eff}}$ plane. The solid curves depict the dependences of the maximum temperature on the white- dwarf mass that follow from the numerical computations (the same as in Fig. 4a). The dashed curves represent the relationships between the effective temperatures and masses of white dwarfs for sources with radii equal to the radii of cool white dwarfs and luminosities that are factors of 4 to 40 lower than the maximum possible luminosity (3). The numbers near the curves indicate the ratio of the luminosity of the white dwarf to the maximum luminosity. The degree of cooling of these three sources at the observation epoch

and the influence of the nonlinearity of the mass — radius relation for white dwarfs are evident (compare the dotted curve in Fig. 4a and the dashed curves in Fig. 4b).

5. Conclusion

We have analyzed archival ROSAT observations of 10 known supersoft X-ray sources, and investigated the source parameters obtained in the first part of our study (Ibragimov et al. 2003) to test for consistency with the model of thermonuclear hydrogen burning on the surface of a white dwarf (vdH92). The values of T_{eff} and $\log g$ obtained for the three hottest sources are consistent with those expected for the stable-burning strip in this model. The parameters of the remaining sources are consistent with those expected for this strip if the lowest possible values of $\log g$ (7.5 - 8.0) are adopted.

We have estimated the sizes and luminosities of ten sources. The sizes and luminosities of two sources (RX J0048 and RX J0439) are not consistent with those for hot white dwarfs, confirming earlier conclusions of other studies that hydrostatic white-dwarf model atmospheres with solar chemical composition are not suitable for these sources. The parameters of another source (RX J0019) are very uncertain, although they lie in the range of admissible parameters for the hot white-dwarf model.

The sizes and luminosities of seven classical super soft sources are in good agreement with the vdH92 model, enabling us to estimate their masses from their sizes and positions in the HR diagram. We considered the dependence of T_{eff} on the mass of the white dwarfs in these supersoft sources and have proposed a formula that can be used to estimate the mass of a white dwarf in a classical binary supersoft source from its temperature.

Acknowledgments

This work was supported by the Russian Foundation for Basic Research (project nos. 99-02-17488 and 02-02-17174).

References

- K. Asai, T. Dotani, F. Nagase, et al., 1998, *Astrophys. J.* 503, L143
- A. Cowley, P. Schmidtke, D. Crampton, and J. Hutchings, 1998, *Astrophys. J.* 504, 854
- B. Gänsicke, A. van Teeseling, K. Beuermann, & D. De Martino, 1998, *Astron. Astrophys.* 333, 163
- B. Gänsicke, A. van Teeseling, K. Beuermann, & K. Reinsch, 2000, *New Astron. Rev.* 44, 143
- J. Greiner, G. Hasinger, & P. Kahabka, 1991, *Astron. Astrophys.* 246, L17
- J. Greiner, R. Schwarz, G. Hasinger, & M. Orio, 1996, *Astron. Astrophys.* 312, 88
- M. Fujimoto, 1982, *Astrophys. J.* 257, 767
- H. Hartmann & J. Heise, 1997, *Astron. Astrophys.* 322, 591
- I. Iben, 1982, *Astrophys. J.* 259, 244
- I. Iben & A. V. Tutukov, 1993, *Astrophys. J.* 418, 343
- I. Iben and A. V. Tutukov, 1996, *Astrophys. J., Suppl. Ser.* 105, 145
- A. A. Ibragimov, V. F. Suleimanov, A. Vikhlinin, & N.A.Sakhibullin, 2003, *Astron. Rep.* 47, 186
- S. Jordan, W. Schmutz, B. Wolff, et al., 1996, *Astron. Astrophys.* 346, 897
- P. Kahabka & E. Ergma, 1997, *Astron. Astrophys.* 318, 108
- P. Kahabka, H. Hartmann, A. Parmar, & I. Negueruela, 1999, *Astron. Astrophys.* 347, L43
- P. Kahabka & E. P. J. van den Heuvel, 1997, *Ann. Rev. Astron. Astrophys.* 35, 69
- M. Kato and I. Hachisu, 1994, *Astrophys. J.* 437, 802
- D. Morgan, 1992, *MNRAS*, 258, 639
- C. Motch, G. Hasinger, & W. Pietsch, 1994, *Astron. Astrophys.* 284, 827
- K. Nomoto, 1982, *Astrophys. J.* 253, 798
- B. Paczynski & A. Zytkov, 1978, *Astrophys. J.* 222, 604
- A. Parmar, P. Kahabka, H. Hartmann, et al., 1997, *Astron. Astrophys.* 323, L33
- R. Popham & R. Narayan, 1995, *Astrophys. J.* 442, 337
- E. P. J. van den Heuvel, D. Bhattacharya, K. Nomoto, and S. Rappaport, 1992, *Astron. Astrophys.* 262, 97

Table 1: Approximation parameters

Object	$N_H,$ 10^{20} cm^{-2}	$T_{\text{eff}},$ 10^5 K	$\log g$ $\text{cm}^2 \text{ s}^{-1}$	$\log (R/d)^2$	Flux 0.2-2 keV $\text{erg}/\text{cm}^{-2}/\text{s}$	$\chi^2/$ d.o.f.
RX J0439.8-6809	5.60	$2.72^{+0.12}_{-0.15}$	7.5	$-26.24^{+0.35}_{-0.26}$	$7.99 \cdot 10^{-11}$	9.30/9
RX J0513.9-6951	7.24	$5.74^{+0.03}_{-0.03}$	8.4	$-28.29^{+0.02}_{-0.01}$	$1.71 \cdot 10^{-10}$	33.8/9
RX J0527.8-6954	6.31	$5.60^{+0.37}_{-1.68}$	9.5	$-29.59^{+0.95}_{-0.14}$	$6.84 \cdot 10^{-12}$	2.01/9
CAL 87	$69.2^{+23.1}_{-22.0}$	$8.20^{+0.22}_{-0.24}$	9.0	$-28.20^{+0.85}_{-0.81}$	$1.17 \cdot 10^{-9}$	13.5/8
CAL 83	6.33	$5.04^{+0.17}_{-0.17}$	8.0	$-28.57^{+0.08}_{-0.08}$	$4.59 \cdot 10^{-11}$	17.3/9
1E 0035.4-7230	6.94	$4.64^{+0.09}_{-0.13}$	8.0	$-28.56^{+0.08}_{-0.05}$	$2.83 \cdot 10^{-11}$	6.10/9
RX J0048.4-7332	$27.6^{+10.5}_{-12.6}$	$3.35^{+0.55}_{-0.48}$	7.5	$-24.55^{+2.82}_{-2.50}$	$3.09 \cdot 10^{-8}$	8.08/8
1E 0056.8-7154	$3.71^{+21.29}_{-2.38}$	$4.00^{+1.24}_{-0.97}$	8.0	$-28.85^{+2.02}_{-0.44}$	$5.31 \cdot 10^{-12}$	13.2/8
RX J0019.8+2156	$16.7^{+6.9}_{-13.35}$	$2.80^{+1.26}_{-0.35}$	7.5	$-23.62^{+2.82}_{-4.67}$	$4.46 \cdot 10^{-8}$	18.1/8
RX J0925.7-4758	163^{+14}_{-46}	$9.85^{+1.05}_{-0.37}$	9.5	$-26.23^{+0.59}_{-1.57}$	$2.53 \cdot 10^{-7}$	8.85/8

Note: The lack of an error for N_H means that this parameter was fixed at the Galactic value. The fluxes were corrected for interstellar absorption.

Table 2: Estimates of physical parameters of the sources

Source	$T_{\text{eff}}, 10^5 \text{ K}$	$\log g$	$R, 10^8 \text{ cm}$	M/M_{\odot}	$L_{\text{bol}}, 10^{37} \text{ erg s}^{-1}$
RX J0513	5.85 ± 0.1	8.0-8.5	8-12	0.8-1.2	5.5-9.5
RX J0527	$5.60^{+0.37}_{-1.68}$	9.0-9.5	2.5-4	1.2-1.4	0.4-0.9
CAL 87	8.2 ± 0.25	8.5-8.75	5-9	1.1-1.3	7.5 - 20
CAL 83	5.04 ± 0.17	8.0-8.25	7-9	0.7-0.9	2.8-3.1
1E 0035	4.64 ± 0.1	7.7-7.9	8-10	0.65-0.85	3-3.3
1E 0056	4 ± 1	7.7-8.5	10-28	0.85-1.05	2.4 - 8
RX J0925	$9.85^{+1}_{-0.4}$	8.5-9.5	5-9	1.2-1.4	4-20

Captions to figures

Figure 1. Position of the sources in the Hertzsprung - Russell diagram. Theoretical relations for white dwarfs with hydrogen burning on their surfaces are also shown: (a) evolutionary tracks for novae in the declining brightness phase (Kato & Hachisu 1994); (b) theoretical curves for stable burning of hydrogen and helium on the surfaces of hot white dwarfs (Iben & Tutukov 1996). The bold solid curve shows the boundary of the stable-burning strip. The numbers near the curves indicate the white-dwarf masses in solar units.

Figure 2. Position of the sources in the $R - \log g$ plane: (a) with specified values of $\log g$ or sizes that are not consistent with those of white dwarfs; (b) with uncertain values of $\log g$. The solid curve shows the theoretical dependence for white dwarfs that follows from the mass - radius relation, and the dashed curve shows the same dependence for the case when the white-dwarf radius is doubled.

Figure 3. Theoretical $M - \log g$ for cool white dwarfs (solid) and for objects with the same masses but doubled radii.

Figure 4. Position of the studied sources in the $T_{\text{eff}} - M$ plane. (a) Position of sources in the stable-burning strip. The dotted curve labeled IT96 corresponds to the theoretical relation proposed by Iben and Tutukov (1996). The solid curves show relations between the maximum temperatures and masses of white dwarfs following from numerical computations of brightness declines of novae (Kato & Hachisu 1994) (upper curve, compare with Fig. 1a) and of stable hydrogen and helium burning on the surfaces of hot white dwarfs (Iben & Tutukov 1996) (lower curve, compare with Fig. 1b). The dashed curve depicts the relation of (6), which we proposed to estimate the masses of white dwarfs with supersoft sources located in the stable-burning strip. (b) Position of sources located on white-dwarf cooling curves. The dashed curves show the dependence of the source temperature on the white-dwarf mass if its radius is equal to the radius of a cool white dwarf with this mass and its luminosity comprises a constant fraction of the luminosity on the plateau (3). The numbers near the curves indicate the luminosity as a fraction of the maximum luminosity on the plateau.

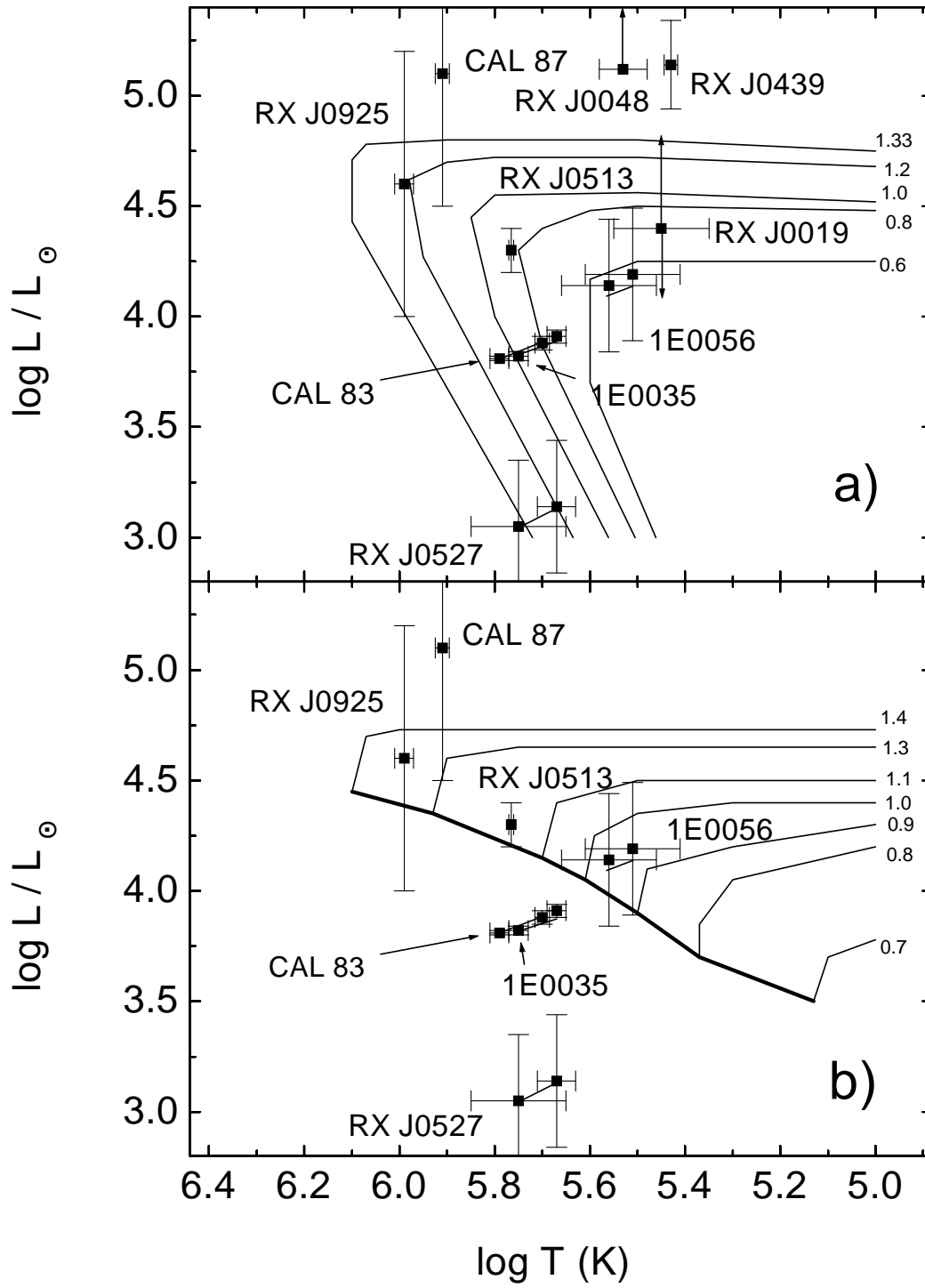


Figure 1:

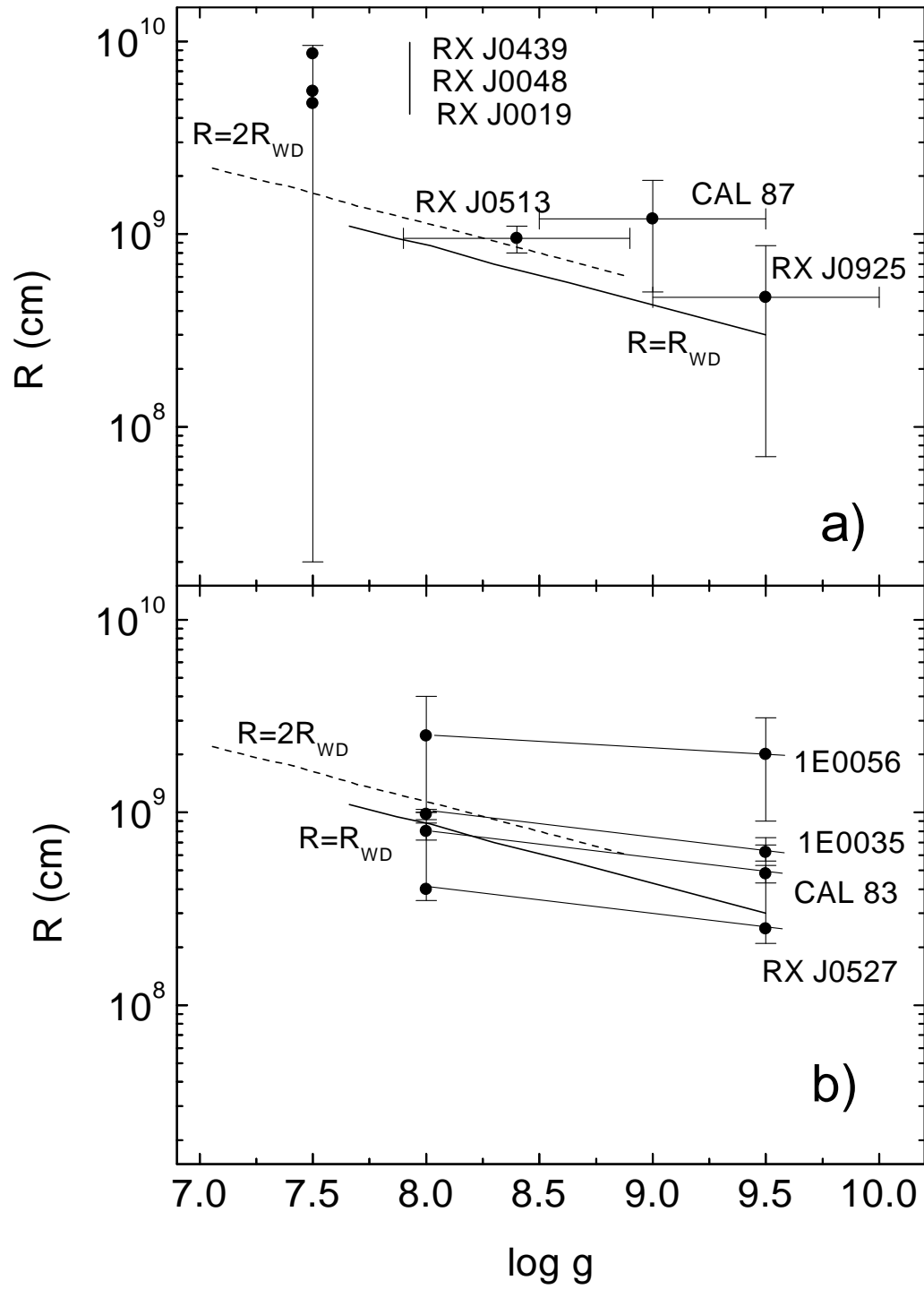


Figure 2:

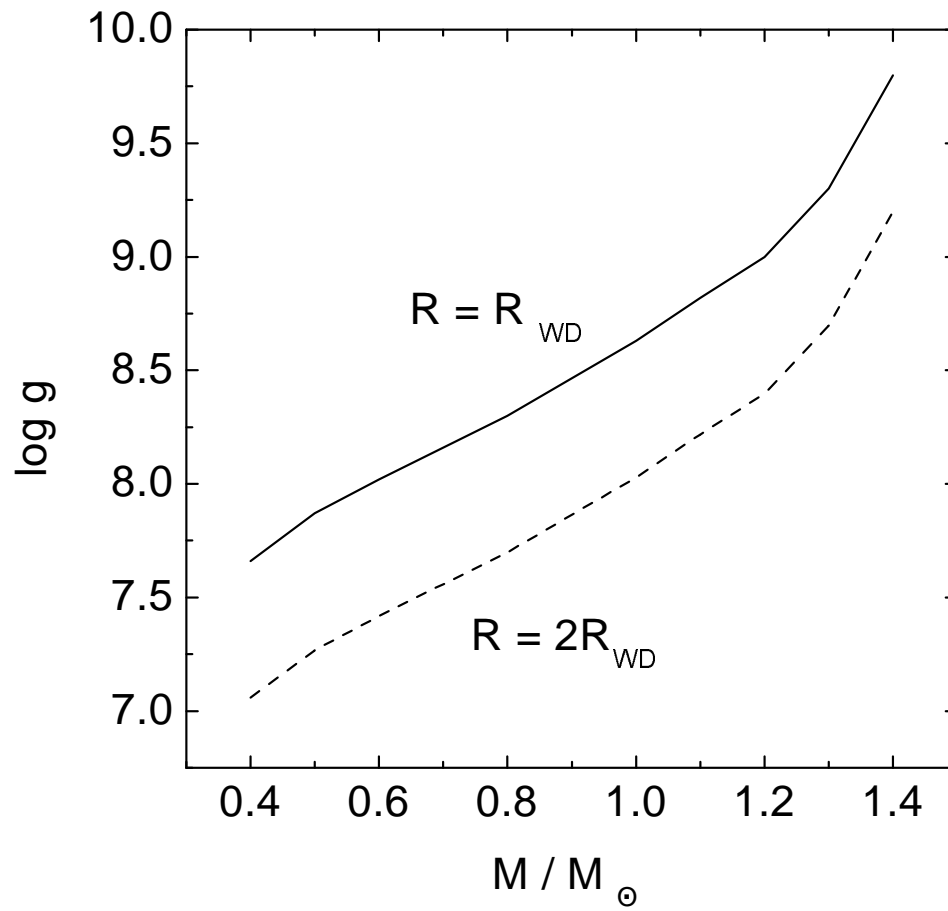


Figure 3:

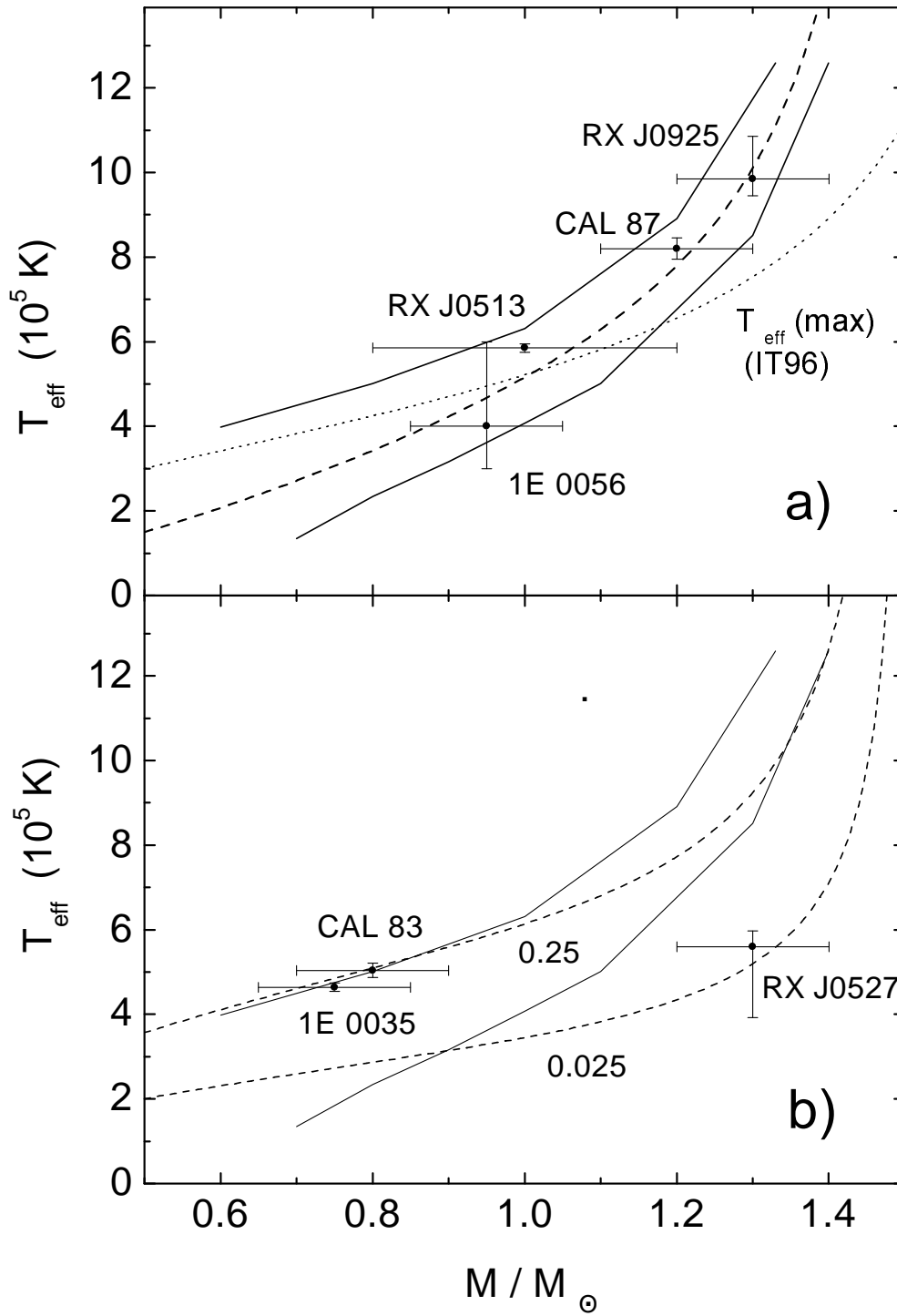


Figure 4: